Jon Sinnreich[1] and Aditya Ayithi[2]

Derivation of p–y Curves from Lateral Pile Load Test Instrument Data

Technical Note

Jon Sinnreich[1] and Aditya Ayithi[2]

Derivation of p–y Curves from Lateral Pile Load Test Instrument Data

Reference

ABSTRACT

Detailed analysis of a bored pile lateral load test is required to generate the family of non-linear lateral load–displacement curves known as "p–y" curves. Current methods of calculating these curves from test pile data may not make full use of all data (inclinometer, strain gage, head deflection) available. The method outlined below incorporates all available data in formulating a mathematical model of the pile behavior from which p–y curves may be derived.

Keywords

lateral load test, p–y curves, bored pile, deep foundation, drilled shaft

Nomenclature

$\{a\}$ = vector of pile behavior model polynomial constant factors

B = total number of measurement data points along Z at a given applied load

C = number of curvature data points along Z at a given applied load

D = number of displacement data points along Z at a given applied load

d = data point depth (units L)

EI = product of Young's modulus E and second moment of area I (units FL^2)

k = Winkler elastic foundation stiffness (units FL)

m = order of the polynomial of the pile behavior model function

M = moment along Z (units FL)

n = degree of derivative of pile behavior model function

N = number of load increments in a static load test

$p =$ line load along Z (units F/L)

$V =$ shear along Z (units F)

$\{q\} =$ vector of measured data points (displacement, rotation, etc.)

$[R] =$ matrix of polynomial operators

$\lambda =$ inverse of pile characteristic length (units 1/L)

$y =$ lateral displacement (units L), dependent function of depth

$Y =$ axis of lateral displacement

$y', y'',$ etc. $=$ first, second, etc., derivative of y with respect to z

$z =$ depth, the independent variable of pile behavior model

$Z =$ axis of depth (positive downward)

$\alpha =$ rotation (units radians) measured by an inclinometer gage

$\varepsilon =$ bending fiber strain measured by a strain gage

$\theta =$ curvature (units 1/L) computed from paired strain gage data

Introduction

Non-linear foundation spring stiffness curves ("p–y" curves) at various depths of a particular site allow the engineer to model the lateral behavior of a pile under various loads. These curves may be constructed based on published empirical methods or derived from lateral pile load testing. When available, p–y curves derived from an on-site load test should provide a better predictor of foundation behavior for that particular site. Previous researchers have presented various methods for deriving p–y curves from a single type of pile test data (typically, inclinometer data), usually using applied load and measured head displacement as boundary conditions. The method presented herein models the pile behavior from a mix of all typical test data (displacements, inclinometers, strain gages, etc., in any available combination), even including applied pile head loads and/or moments, which themselves may be considered to be measured data points.

Background

To determine the lateral capacity of the pile, p–y curves are used to represent nonlinear springs attached at nodes along the length of the pile in a numerical model of the soil–structure interaction. McClelland and Focht (1958) developed the concept of p–y curves, in which the lateral soil reaction per unit length p is plotted versus the pile displacement y at discrete depths. Other important work on theoretical solutions and instrumentation was developed by Matlock et al. (1956), Matlock and Ripperger (1958), and Matlock and Reese (1962).

The elementary analytical model used for the behavior of a laterally-loaded pile is the semi-infinite beam on a Winkler foundation. The model is defined on a coordinate system with origin at the ground elevation. The depth variable z increases downward along the Z-axis, which lateral displacement y is measured along the Y-axis (see **Fig. 1**). The basic differential relationship from beam theory is expressed as:

$$(1) \qquad EI\frac{d^4y}{dz^4} + ky = 0$$

where:

$EI =$ the beam bending stiffness,

$k =$ the elastic foundation spring stiffness, and

$y = f(z) =$ a continuous, differentiable function of depth.

Multiplying the second, third, and fourth derivative of this displacement function, respectively, by EI yields functions for the moment M, shear V, and line load p, respectively:

$$(2) \qquad M = EI\frac{d^2f(z)}{dz^2}$$

$$(3) \qquad V = EI\frac{d^3f(z)}{dz^3}$$

$$(4) \qquad p = EI\frac{d^4f(z)}{dz^4}$$

If both EI and k are constants, closed-form solutions to Eq 1 have been derived for a number of boundary conditions, including an applied point load and applied moment at the free end of a semi-infinite beam, which are of greatest interest in modeling a laterally-loaded pile (Hetényi 1946). For the case of an applied pile head lateral load P_0, y is computed as:

$$(5) \qquad y = e^{-\lambda z}\frac{2\lambda P_0}{k}\cos(\lambda z)$$

where

$$(6) \qquad \lambda = \sqrt[4]{\frac{k}{4EI}}$$

is a constant of units 1/L, known as the inverse of the *characteristic length* of the beam. A closed-form solution has also been put forward for the case of a foundation stiffness monotonically increasing with depth $k(z) = k_0 z$ (Franklin and Scott 1979). However, more complicated problems involving foundation stiffness which is variable not only with depth, but also with

FIG. 1   Conceptual sketch of lateral pile forces and reactions.
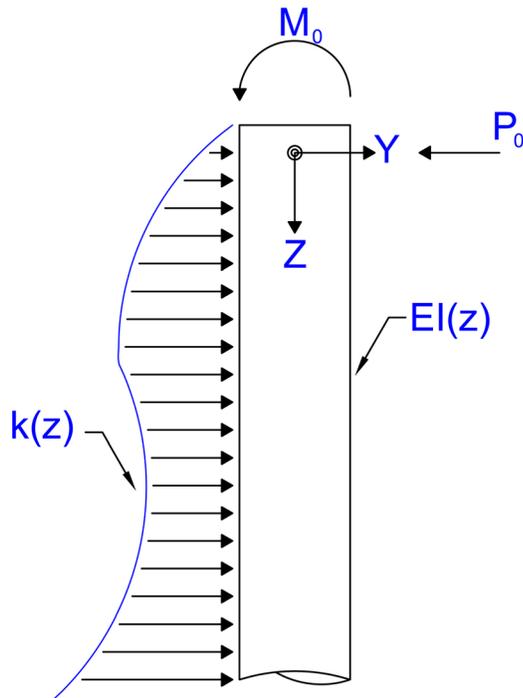
displacement (non-linear stiffness curve), especially if combined with a variable EI (due to changes in pile reinforcement and/or diameter along the pile length, or because of tensile cracking due to applied load), do not have closed-form solutions available.

Accurate determination of p–y curves directly from a lateral pile load test is desirable for input into numerical analysis and design programs (for example the COM624P code or its commercial derivative LPILE; see Wang and Reese (1993), or FB-MultiPier), but not straightforward. Typically, instruments are embedded in the test pile to ascertain behavior under load. These instruments are located at relatively few discrete depths, which may not correspond to the points of inflection, maximum bending, etc., which would be of greatest interest in characterizing the pile response to load. Fitting of analytical curves to discrete data points is a method to cope with these limitations. Once an analytical function is curve-fit to the data, it may be used to investigate pile behavior at any depth.

Many authors (for example McVay et al. (2009), Nip and Ng (2005)) have implemented curve fitting to lateral load test data, using the assumption that the function $f(z)$ can be approximated by a polynomial of sufficiently high order m:

(7)
$$y = f(z) \approx \sum_{i=0}^{m} a_i z^i$$

This assumption has the advantage that a solution may be obtained via the method of linear least-squares (LLS), which is easily implemented. The LLS method is based on the construction of a set of polynomial equations:

(8)
$$[R]\{a\} = \{q\}$$

where the $B \times (m+1)$ matrix $[R]$ consists of B number of rows of polynomial operator vectors $\{ 1, \quad z, \quad z^2, \quad \cdots \quad z^m \}$ on the independent variable z, the vector $\{a\} = \{ a_0 \quad \cdots \quad a_m \}^T$ contains the constant factor for each corresponding operator, and the vector $\{q\} = \{ y_1 \quad \cdots \quad y_B \}^T$ contains the B number of measured data points. To implement the LLS, the number of data points must be greater than or equal to the order of the polynomial plus one: $B \geq (m+1)$. Equation 8 is reformulated as:

(9)
$$[R]^T[R]\{a\} = [R]^T\{q\}$$

then solved for $\{a\}$:

(10)
$$\{a\} = \left[[R]^T[R] \right]^{-1} \left\{ [R]^T\{q\} \right\}$$

One disadvantage is that subsequent derivatives of the polynomial function geometrically compound any errors in the original curve-fit. Taking the fourth derivative of Eq 7 can result in nonsense when plugged back into Eq 1. To overcome this, one theoretical solution is to increase the order of the polynomial. The exponential and trigonometric components of Eq 5 may both be expressed as Taylor series, and thus their product should be amenable to accurate approximation by polynomials; however, in order to match Eq 5 over a range of $0 \leq \lambda z \leq \pi$ to 0.01 %, a 15th-order polynomial is required. This value may easily exceed the number of available data points B (the problem becomes underdetermined, and thus is not suitable for a LLS curve fit). Therefore, the method of a purely polynomial approximation may be of limited use in extracting the p–y curves from test data. As one possible alternative, Brown et al. (1994) proposed refining assumed p–y curves by optimizing the input parameters of a computer model until the model output matches inclinometer data. This approach makes indirect use of the inclinometer data but does not include other potential data sources such as strain gages. Other proposed methods for back-calculating p–y curves include the b-splines curve-fitting (de Sousa Coutinho 2006) and residual numerical differentiation method (Brandenberg et al. 2010).

Curve-Fit Method Formulation

The method of analysis proposed herein modifies the standard polynomial function of Eq 7 by addition of an exponential multiplier, similarly to Eq 5:

$$y = e^{-\lambda z} \sum_{i=0}^{m} a_i z^i \tag{11}$$

which serves to dampen out the amplitude of $f(z)$ and its derivatives at greater depths, analogous to the structure of Eq 5.

In compact form, the nth derivative of this function with respect to z can be written as:

$$\frac{d^n f(z)}{dz^n} = e^{-\lambda z} \left\{ \sum_{j=0}^{n} \left(\frac{n!}{j!(n-j)!} \right) (-\lambda)^{(n-j)} \right. \\ \left. \times \left\{ \sum_{i=j}^{m} \left(\frac{i!}{(i-j)!} \right) a_i z^{(i-j)} \right\} \right\} \tag{12}$$

Note that if λ is set equal to zero in Eq 12, the original simple polynomial of Eq 7 (and its derivatives) is recovered. Next, Eq 12 is rearranged to group terms by the polynomial constants a_i:

$$\frac{d^n f(z)}{dz^n} = \sum_{i=0}^{m} a_i e^{-\lambda z} \sum_{j=0}^{b=\min(i,n)} \\ \times \left\{ (-\lambda)^{(n-j)} \left(\frac{n!}{j!(n-j)!} \right) \left(\frac{i!}{(i-j)!} \right) z^{(i-j)} \right\} \tag{13}$$

Data collected during the course of a lateral load test is unusual in that some of the measured data (lateral displacement) may be modeled using the assumed mathematical function y, while other measured data (rotation α, curvature θ) may be modeled using *derivatives* of the same function y:

$$\alpha_d = dy_d/dz = y'_d; \quad \theta_d = d^2 y_d/dz^2 = y''_d$$

The proposed curve-fit method incorporates all of these data into a single LLS, which will find the best-fit function to match displacements, while simultaneously matching rotation and curvature data with derivatives of the same function.

In-place inclinometer (IPI) instruments are typically preferred for lateral load tests since they can be sampled nearly instantaneously at multiple fixed depths, numerous times over the course of a test. IPI data measures rotation α_d at discrete depths z_d (in radians). This is used to calculate a lateral pile displacement profile via numerical integration, by summing the sine of each measured rotation multiplied by the spacing between the IPI gages. Because the casing bends continuously, but in-place inclinometers pivot at fixed points, the measure of rotation α_1 given by the gage is not valid at the gage pivot point elevation z_1, but rather at some lower elevation z_2 (see **Fig. 2**) which is not explicitly known. Therefore, data from IPIs should be converted to calculated displacement y_d rather than the measured rotation α_d, using simple trigonometry and the assumption that the base pivot wheel of the IPI string ("IPI 0") does not translate laterally. Pile head lateral dial gages or displacement transducer (DT) gages provide an independent measurement of lateral head translation, which may also be used to

FIG. 2   IPI point of rotation schematic.
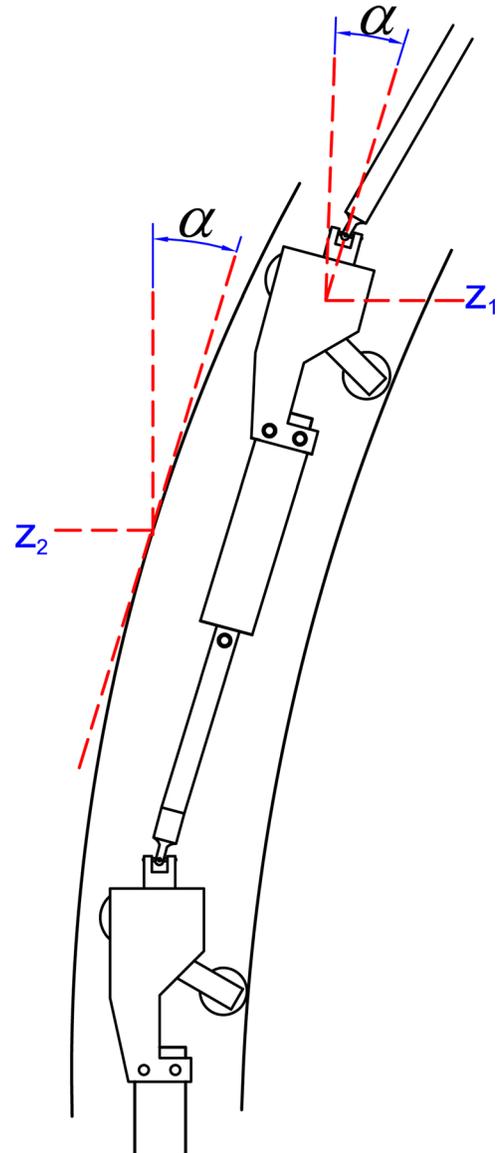
determine if the base pivot point of the inclinometer string is fixed by comparing the measured DT and computed IPI displacements at ground elevation. Thus, inclinometers and pile head displacement transducers are both used to generate displacement data points y_d at depths z_d.

An inclinometer which provides rotation data at the exact depth of the instrument, such as a single instrument lowered into the casing on a cable and sampled sequentially at different depths, will generate rotation data points y'_d at depths z_d.

Strain gages (SGs) in opposing pairs, aligned vertically in the pile in the plane of the direction of lateral loading at a radius r from the centerline, provide curvature data:

$$\theta_d = \frac{\left(\varepsilon_{\text{compression}} - \varepsilon_{\text{tension}} \right)_d}{2r} \tag{14}$$

Note that Eq 14 assumes the pile is axi-symmetric, and the bending stiffness EI remains constant (concrete has not fractured on the tensile side and the neutral axis is at the center of the pile). It may be possible to analyze paired strain gage data beyond the tensile strain limit to compute θ using an appropriate model for a variable EI and changing neutral axis location. For the sake of simplicity in illustrating the proposed curve-fitting method, the assumption is made throughout this discussion that the pile remains intact, and that the bending stiffness EI is also constant.

To demonstrate the proposed method, assume that D number of inclinometer displacement data points (z_1, y_1) to (z_D, y_D), plus C number of strain gage curvature points (z_1, y_1'') to (z_C, y_C'') are available from a lateral load test. In order to implement the least squares fit, $(D + C)$ must be greater than or equal to m (the problem must be overdetermined).

First, the $(D + C) \times (m + 1)$ matrix array $[R]$ is constructed of the model components for each data point:

(15)
$$[R] = \begin{bmatrix} g_{1,0} & \cdots & g_{1,m} \\ \vdots & \ddots & \vdots \\ g_{D,0} & \cdots & g_{D,m} \\ \hline h_{1,0} & \cdots & h_{1,m} \\ \vdots & \ddots & \vdots \\ h_{C,0} & \cdots & h_{C,m} \end{bmatrix}$$

with the elements:

i. $g_{d,i} = e^{-\lambda z_d}(z_d)^i$ (from Eq 11)

ii. $h_{d,i} = e^{-\lambda z_d} \sum_{j=0}^{b=\min(i,2)} \left\{ (-\lambda)^{(n-j)} \left(\frac{n!}{j!(n-j)!} \right) \left(\frac{i!}{(i-j)!} \right) z^{(i-j)} \right\}$

(from Eq 13)

Next, a $(D + C) \times 1$ vector array of the observed data points is constructed:

(16)
$$\{q\} = \{ y_1 \quad \cdots \quad y_D \quad | \quad y_1'' \quad \cdots \quad y_C'' \}^T$$

The LLS is then solved using Eq 10. The resulting vector array $\{a\}$ contains the $(m + 1)$ polynomial constants that result in a simultaneous best fit for the given D displacement and C curvature data points, for a given inverse characteristic length λ. Because λ is non-linear with respect to the variable z, it cannot be determined directly via the LLS. A value may be picked by the user which yields reasonable results (see discussion in Case 1 Validation, below), or it may be optimized either by use of a non-linear Gauss–Newton solution in a program implementation (an iterative optimization), or by use of an optimization package in a spreadsheet implementation, (i.e., Solver in Microsoft Excel).

Once all constant parameters $\{a\}$, λ have been determined, Eqs 11 and 12 may be used to compute the curve-fit displacement and its derivatives, and the moment, shear, and line-load profiles are recovered using Eqs 2–4.

Additional sources of data besides IPIs and SGs may also be considered. An inclinometer attached directly to the pile head will provide a head rotation data point y_0'. The known applied load P_0, and moment M_0 (applied directly or generated implicitly if P_0 is applied to a free-standing column some distance above the origin) may be used to generate two additional data points $y_0''' = P_0/EI$ and $y_0'' = M_0/EI$, respectively. For deeply-embedded piles, displacement, rotation, moment (curvature), shear, and line load may all be assumed zero at the pile tip. This data can also be directly incorporated into the curve fit. Note that in other formulations (Nip and Ng 2005), inputs such as head displacement, head rotation, applied moment, and shear at the head and zero moment and shear at the tip are considered boundary conditions which must be satisfied exactly. In the current proposed solution scheme, they are considered additional data points, which contribute to the solution but may not be precisely matched by the curve-fit. Considering that most such data points are themselves either assumptions or measurements with their own associated uncertainties, it does not seem unreasonable to give them roughly equal weight as inclinometer and strain gage data points. Additionally, a further possible refinement to the solution is the addition of a weighting matrix, by which the user can assign different weights to different data points (based on confidence of various data's accuracy, for instance):

(17)
$$\{a\} = \left[[R]^T [w][R] \right]^{-1} \left\{ [R]^T [w]\{q\} \right\}$$

The default value for $[w]$ is the identity matrix [I], giving equal weight to each data point. To construct a p–y curve at a given depth, the solution outlined above is implemented for each of a series of load test increments 1 to N, resulting in N sets of constant vectors $\{a\}_1$ to $\{a\}_N$. Next, for each load increment, Eq 4 and Eq 11 are solved at the selected depth, and the results tabulated.

As mentioned above in the discussion of strain gage data, the bending stiffness EI is assumed constant in the derivation presented above and the validation calculations in the next section (justified by the fact that in the pile in Case 1, embedded strain gage data yielded the same magnitude of bending strain on the compressive and tensile sides, and in Case 2 is a simple virtual model). In a typical reinforced concrete pile, lateral loading will result in tension cracks developing, leading to an EI that is a non-linear function of strain. This function may be approximated by application of the relevant beam theory and does not preclude the use of this method to calculate M, V, or p using Eqs 2–4, simply by replacing EI with $EI(\varepsilon)$. However, it should be noted that the additional assumptions associated with modeling EI as a function of strain will introduce more uncertainty into the analysis.

Validation

CASE 1

The first data set used for validation of the method outlined above is one of the very few known to the author to include direct measurement of lateral pressures in a full-scale lateral pile test. **Figure 3** illustrates the lateral instrumentation schematic for a pile load test conducted in Friedetal, Germany (Loadtest 2006). The test was conducted as part of the construction of a viaduct on the Göttingen-to-Halle autobahn A38 highway. This viaduct, which crosses the Peace Valley (the "Friedetal") near Sollstedt in the state of Thüringen, has a total span of 485 m formed in six sections with the largest spanning 130 m. The ground conditions at the site were quite challenging, with gypsum layers susceptible to washout plus the potential of subsistence due to a history of mining in the region.

The 1180-mm diameter test pile was excavated dry to a depth of −47.81 meters by oscillating a sectional temporary casing downward and removing the soil with a crane operated grab. After reaching tip elevation, the rebar cage (eight 25-mm epoxy-coated steel vertical rebars with 10-mm epoxy-coated steel hoops at 250 mm spacing) with attached instrumentation was inserted simultaneously with a permanent 26-m long, 1016-mm O.D., 16-mm thick steel casing coated on the outside with bitumen. The permanent casing was installed to isolate the upper pile section from down-drag due to anticipated soil settlement. Concrete was delivered by pump through a nominal 150-mm pump line inserted to the base of the pile. As the concrete head rose above the base of the permanent casing, grout was pumped into the annulus between the permanent and temporary casings through a nominal 13-mm pipe. Sections of temporary casing and pump line were removed as the concreting progressed until reaching the concrete cutoff elevation at the ground surface.

Six specially-made piezometer lateral earth pressure cells (PCs) with dimensions 150 mm wide by 200 mm tall were

FIG. 3

Friedetal test pile schematic.
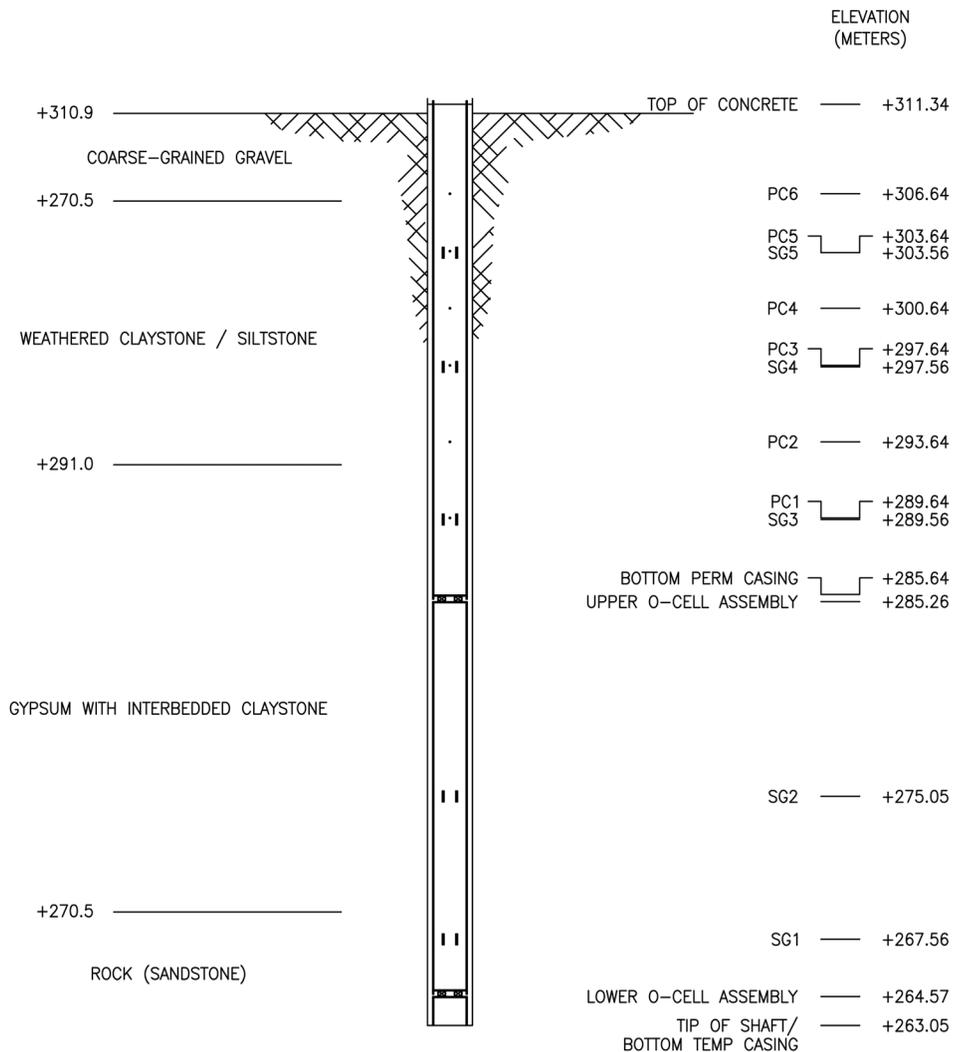
TABLE 1 Friedetal lateral test data summary.

Load Increment	Load (kN)	Inclinometers (degrees)						
		1	2	3	4	5	6	7
1L-1	120	−0.005	−0.003	−0.012	−0.002	−0.005	0.007	0.032
1L-2	240	−0.006	−0.004	−0.020	−0.013	−0.010	0.021	0.056
1L-3	360	−0.007	−0.004	−0.025	−0.006	−0.007	0.033	0.087
1L-4	480	−0.007	−0.004	−0.029	−0.007	−0.004	0.045	0.123
1L-5	600	−0.008	−0.005	−0.033	−0.009	−0.002	0.063	0.165

Load Increment	Load (kN)	Head Display (mm)	Pressure Cells (kPa)					
			1	2	3	4	5	6
1L-1	120	1.56	−5.7	0.0	1.3	−15.6	−11.0	60.1
1L-2	240	4.20	−4.6	−0.8	−0.1	−32.5	−7.2	91.7
1L-3	360	7.43	−11.2	−2.1	−6.1	−53.9	6.9	119.8
1L-4	480	11.01	–	−4.1	−15.8	−76.7	24.8	154.4
1L-5	600	15.42	–	−3.9	−15.9	−78.1	24.7	152.4

Load Increment	Load (kN)	Strain Gages (microstrain, C = compression, T = tension)									
		1C	1T	2C	2T	3C	3T	4C	4T	5C	5T
1L-1	120	−0.8	−0.5	−0.5	−0.2	0.1	0.1	−0.2	0.4	6.8	−5.7
1L-2	240	−1.6	−1.0	−0.4	−0.4	0.5	0.2	−0.9	1.4	21.9	−19.5
1L-3	360	−2.2	−1.5	−0.6	−0.6	0.1	0.1	−2.5	1.9	41.3	−38.1
1L-4	480	−3.2	−1.9	−0.8	−0.8	−0.2	−0.3	−4.3	2.6	63.2	−59.2
1L-5	600	−3.5	−2.4	−1.0	−0.9	−0.4	−0.6	−6.9	3.3	89.2	−83.3

installed in the wall of the permanent casing during construction, in line with the direction of applied lateral load. A string of IPIs (not illustrated) was inserted into a cast-in-place casing prior to start of the test, with an inclinometer at each lateral pressure cell elevation. Five levels of paired sister-bar SGs in line with the lateral load were attached to the reinforcing cage. All embedded instruments used in the test were vibrating-wire type gages, with individual calibrations performed prior to installation in the pile. The test pile was laterally loaded in five nominally equal steps (designated "1L-1" to "1L-5") to a maximum load of 600 kN. Because the test pile had been used previously as an axial test pile, with two levels of embedded Osterberg cells (Osterberg 1989), the lateral analysis is only carried out down to the upper Osterberg cell (O-cell) elevation. The previously-expanded upper O-cell (which was not pressurized during the lateral test) acted as a pivot which would not transmit moment, and only partially transmit shear. The test section of the pile is therefore approximately 26 ms deep, although the entire pile was approximately 48 ms deep. The lateral load was applied in tension via a 50-mm steel bar cored through the pile approximately 0.2 meters above ground elevation and connected to a reaction pile. Data collected during the course of the load test and used in the calculations below is summarized in **Table 1**.
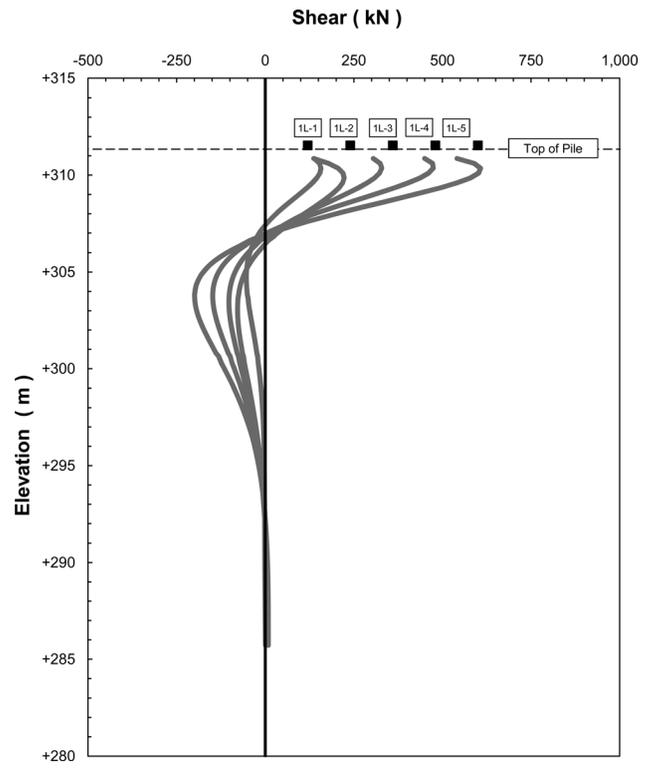
The 0.15-m wide pressure cells were located in-line with the direction of load application, and measured pressure in kPa

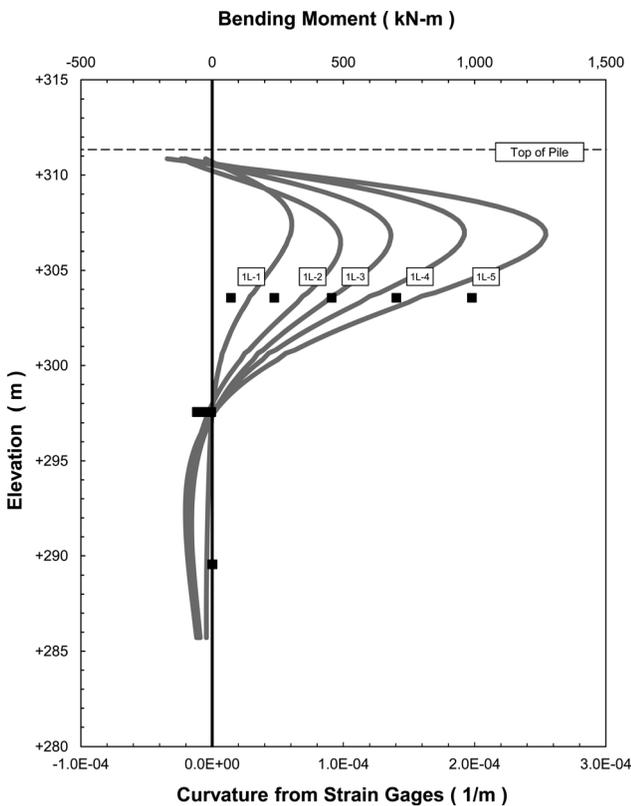**FIG. 4** Friedetal lateral test displacement data and curve-fit.
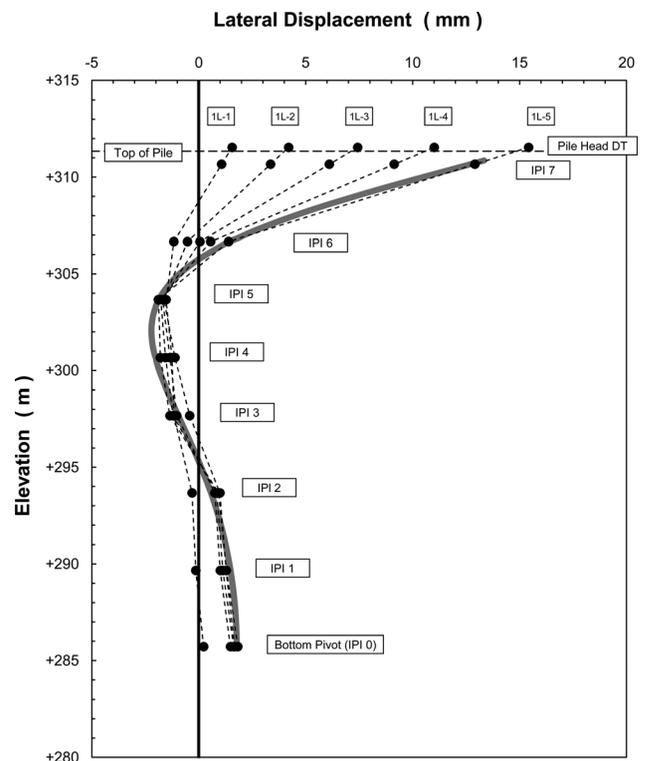
FIG. 5   Friedetal lateral test line load data and curve-fit.
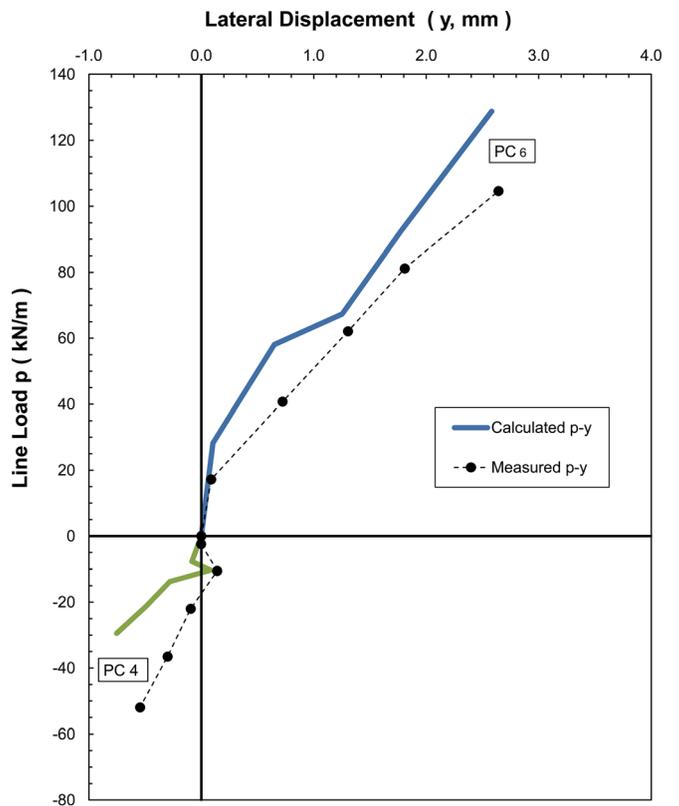

Lateral Line Load (kN/m)
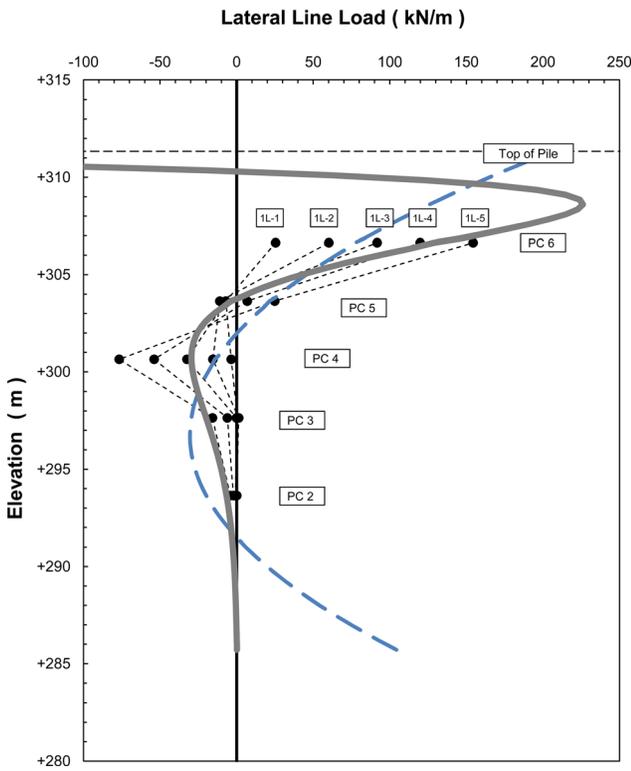
FIG. 7   Friedetal lateral test computed shears.

Shear (kN)

FIG. 6   Friedetal lateral test strain gage curvature and computed moments.

Bending Moment (kN-m)

Curvature from Strain Gages (1/m)

FIG. 8   Friedetal lateral test measured and computed p–y curves.



Lateral Displacement (y, mm)

on the central 15 % of the 1.016-m wide pile cross-section only. In order to convert the measured pressure into a line load on the whole pile face, in units of kN/m, the results were multiplied by the pile diameter, then scaled by two-thirds, based on the assumption of a parabolic pressure distribution on the cross-section of pile diameter (see Prasad and Chari 1999). For this data set, it was possible to estimate $\lambda = 0.255$ based on the slope of the measured p–y curve at Pressure Cell 6 (PC 6) and the computed pile EI of 2307 MN-m^2, using Eq 6. Use of a constant EI for this analysis is justified by the observation that the tensile and compressive strains recorded up to maximum applied load are of equal magnitude (**Table 1**), indicating uniform curvature in the pile and the absence of tensile cracks, at least up to the elevation of the top-most level of strain gages. The polynomial order m was selected to be 6 in order to minimize fitting errors.

Data used in the curve-fit included IPI 0 to 7, SG 3 to 5 (the levels above the upper O-cell), the Pile Head DT, and the shear (applied load divided by EI) and moment (zero) at the pile head, for a total of 14 data points. Note that all gage positions are numbered sequentially from deepest embedment to shallowest, following the convention of bi-directional axial (O-cell) load test instrumentation schematics. Based on the load test data, the curve-fit function parameters discussed above and the analysis technique described in the previous section, the following results were obtained:

Figure 4 plots the computed lateral deflections, based on IPI and Pile Head Displacement Transducer (DT) data, for each load increment 1L-1 to 1L-5. The measured data points are connected by dashed lines to indicate assumed displacement curves. The grey line is the curve-fit displacement result for 1L-5

FIG. 9

Split-lateral test program schematic.
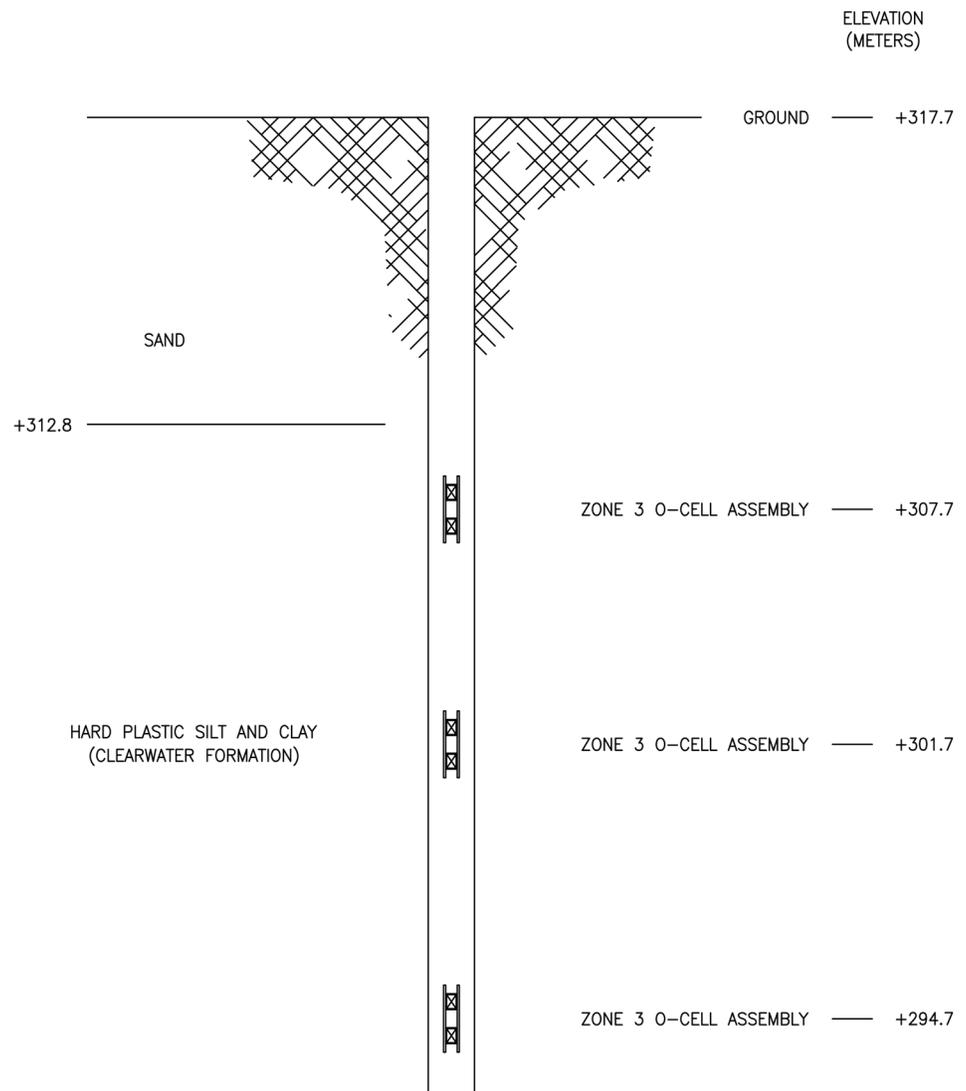
(results were computed for each load increment, but omitted in **Figs. 4** and **5** for clarity).

Figure **5** plots the computed line load from PCs, and the curve-fit result for 1L-5. Note that PC 1 gave unusually high results, then stopped functioning altogether, and is not included in the plot or any data analysis. For comparison purposes, the thick grey dashed line is the result of an identical analysis but with $\lambda = 0$ (simple polynomial). A simple visual inspection of this result clearly indicates that it is a very poor fit to the measured PC data, most likely due to the accumulated errors of differentiating a simple polynomial fit four times.

Figure **6** plots the measured curvature from Strain Gage levels 3, 4, and 5 (data points) and the computed bending moment (curves). **Figure 7** plots the computed shear profiles. Finally, the measured (dashed line) and computed (solid line) p–y curves at PC levels 4 and 6 (the only two levels where significant displacement occurred) are compared in **Fig. 8**.

Note that there is not perfect correlation between all measured data points and curve-fit results. In particular, the cure-fit curvature at SG 5 elevation is approximately 75 % greater than what was derived from the strain gages. These discrepancies may be due to limitations of the method, the assumption of a constant *EI* and/or the assumptions made in converting sister-bar axial strain data into a curvature value (Eq **14**). Also note that the displacement axis in **Fig. 9** has been offset by 1.25 mm to account for initial displacement due to previous testing. The apparent lateral displacement at the tip of the upper pile section (**Fig. 4**), computed by offsetting the IPI results to match pile head DT data, may indicate a shear load transfer through the upper O-cell, although there is no way to confirm or quantify this with the available instrumentation. O-cell hydraulic seals have a certain amount of play to allow an O-cell to maintain pressure without binding up if differential opening due to non-symmetric reaction occurs during a bi-directional test. The negative line load for PC 4 is due to the displacement reversal, and may not be an adequate match partly because the pressure cell was on located on the "wrong" (i.e., tensile) side of the pile due to the reversal. Nevertheless, the curve-fitting method is able to recover, to a reasonable degree, the magnitude of both line load and displacement (the "p" and the "y," respectively, of the measured p–y curves). Note that the actual PC data was not included in the curve-fitting, since it was being used as the validator of the method in this case, although it *could* have been included by using the appropriate application of Eq **13**.

CASE 2

The second data set used for validation of the method outlined above comes from a series of three split-lateral tests conducted on a site in Canada (Loadtest 2010). The split-lateral test is a specialized full-scale test designed to measure lateral soil resistance at a specific depth (Brown and Camp 2002). For this project, the engineer needed to isolate the lateral load carrying capacities of a deeper soil formation for design purposes because the overburden layers would be cut as a part of the construction project and would not contribute to pile capacity.

The three tests were conducted in adjacent excavations, at depths of 10, 16, and 23 ms (designated as Zones 3, 2, and 1 in the test results), respectively. **Figure 9** illustrates a composite schematic showing the relative positions of each assembly in a single vertical axis for clarity, relative to the soil profile. The data were used as input to solve for eight load steps in a

TABLE 2   Split-lateral test data summary.

Zone 3		Zone 2		Zone 1	
Y (m)	P (kN/m)	Y (m)	P (kN/m)	Y (m)	P (kN/m)
0.000	0	0.000	0	0.000	0
0.001	284	0.001	432	0.001	820
0.002	546	0.002	826	0.002	1408
0.003	790	0.003	1187	0.003	1851
0.004	1017	0.004	1519	0.004	2195
0.005	1228	0.005	1825	0.005	2472
0.006	1426	0.006	2108	0.006	2698
0.007	1611	0.007	2371	0.007	2887
0.008	1785	0.008	2616	0.008	3047
0.009	1948	0.009	2844	0.009	3184
0.010	2102	0.010	3058	0.010	3303
0.011	2248	0.011	3258	0.011	3407
0.012	2385	0.012	3446	0.012	3499
0.013	2515	0.013	3622	0.013	3581
0.014	2639	0.014	3789	0.014	3654
0.015	2756	0.015	3946	0.015	3720
0.016	2868	0.016	4095	0.016	3780
0.017	2974	0.017	4236	0.017	3834
0.018	3075	0.018	4369	0.018	3884
0.019	3171	0.019	4496	0.019	3929
0.020	3264	0.020	4617	0.020	3971

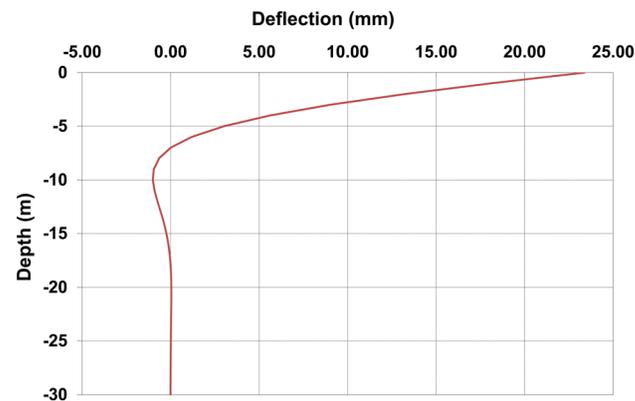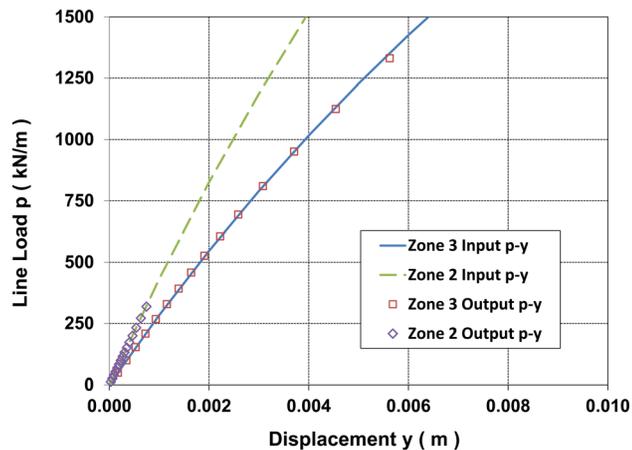**FIG. 10**   Split-lateral test computed lateral deflection.

FIG. 11 Split-lateral test input and output p-y curves.

Microsoft Excel implementation of the COM624P lateral pile analysis program (Jenkins 2010), using a pile *EI* of 16000 MN-m^2 derived from an assumed 1.525-m diameter pile design (no actual pile was constructed during the testing phase, only three separate split-lateral assemblies).

Table **2** lists the three p–y curves derived from the split-lateral tests (curves are smoothed for analysis purposes):

A typical load–displacement response is plotted in **Fig. 10**. The resultant eight load–displacement profiles were then used as input into the curve-fit algorithm, the results of which were reconstructed into p–y curves as described above. For this analysis, λ was estimated to be equal to 0.3 using Eq **6** and based on the pile *EI* and average modulus *k* derived from the split-lateral results. The polynomial order *m* was selected to be 7 in order to minimize fitting errors. Zone 1 (the deepest, at 23 ms) did not experience any significant movement in the COM624P model, but Zones 2 and 3 did, with excellent matching between the input and output p–y curves, as plotted in **Fig. 11**.

Conclusion

A new method of curve-fitting data analysis for a lateral load pile test is proposed that includes the calculation of p–y curves from all available instrument data typically gathered during such a test. Validation against real pile test results yields good comparisons. In Validation Case 1, while the p–y results are not an exact match, they do provide values which may be considered adequate given the necessary assumptions made in the analysis and amount of uncertainty in measured data. The results plotted in **Figs. 5** and **7** also conform to the expectation that moment should be zero at the pile head, and then increase with depth until soil reaction dampens it out, while the shear curves generally match the magnitudes of loads applied at the pile head. In Validation Case 2, the output p–y curves match the input p–y curves closely.

The method outlined in this paper is not fully automatic, and requires the user to employ some engineering judgment in selecting the input parameters λ and *m*, such that the results conform to the general expectations of pile behavior. However, the solution is direct, not iterative, and can be implemented in a spreadsheet format relatively easily, which allows for straightforward analysis of test results for input into design methods.

The addition of a variable flexural stiffness *EI* (due to flexural cracking of pile concrete, typically) introduces an additional complication in the analysis which is not addressed in this paper. It is hoped that further research, by the authors or others, will extend the method to piles with variable flexural stiffness.

References

Brandenberg, S. J., Wilson, D. W., and Radhid, M. M., 2010, "Weighted Residual Numerical Differentiation Algorithm Applied to Experimental Bending Moment Data" *ASCE J. Geotech. Geoenviron. Eng.*, Vol. 136, No. 6, pp. 854–863.

Brown, D. A., Hidden, S. A., and Zhang, S., 1994, "Determination of p–y Curves Using Inclinometer Data," *ASTM Geotech. Test. J.*, Vol. 17, No. 2, pp. 150–158.

Brown, D. A. and Camp, W., 2002, "Lateral Load Testing Program for the Cooper River Bridge, Charleston, SC" *Proceedings of the ASCE Deep Foundations 2002 Conference Proceedings*, Orlando, FL, Feb 14–16.

de Sousa Coutinho, A. G. F., 2006, "Data Reduction of Horizontal Load Full–scale Tests on Bored Concrete Piles and Pile Groups," *ASCE J. Geotech. Geoenviron. Eng.*, Vol. 132, No. 6, pp. 752–769.

Franklin, J. N. and Scott, R. F., 1979, "Beam Equation with Variable Foundation Coefficient," *J. Eng. Mech. Div.*, Vol. 105, No. 5, pp. 811–827.

Hetényi, M., 1946, *Beams on Elastic Foundation*, University of Michigan Press, Ann Arbor, MI.

Jenkins, D., 2010, "LatPilePY.xls," http://interactiveds.com.au (Last accessed 14 Oct 2013).

Loadtest Inc., 2006, *Data Report Reference No. 533 (Friedetal, Germany)*, Osterberg Cell Load Test Database, Gainesville, FL.

Loadtest Inc., 2010, *Data Report Reference No. 676 (Ft. McMurray, AB)*, Osterberg Cell Load Test Database, Gainesville, FL.

Matlock, H., Ripperger, E. A., and Fitzgibbon, D. P., 1956, "Static and Cyclic Lateral Loading of an Instrumented Pile," *Report to Shell Oil Company*, Shell Oil, Austin, TX.

Matlock, H. and Ripperger, E. A., 1958, "Procedures and Instrumentation for Tests on a Laterally Loaded Pile," *Proceedings of the 8th Texas Conference on Soil Mechanics and Foundation Engineering*, University of Texas, Austin, TX.

Matlock, H. and Reese, L., 1962, "Generalized Solutions for Laterally Loaded Piles," *Trans. Am. Soc. Civ. Eng.*, Vol. 127, pp. 1220–1246.

McClelland, B. and Focht, J., 1958, "Soil Modulus for Laterally Loaded Piles," *Trans. Am. Soc. Civ. Eng.*, Vol. 123, pp. 1049–1086.

McVay, M. C., Wasman, S. J., Consolazio, G. R., Bullock, P. J., Cowan, D. G., and Bollman, H. T., 2009, "Dynamic

Soil–Structure Interaction of Bridge Substructure Subject to Vessel Impact," *J. Bridge Eng.*, Vol. 14, No. 1, pp. 7–16.

Nip, D.C. N. and Ng, C. W. W., 2005, "Back–Analysis of Laterally Loaded Bored Piles," *Proc. Inst. Civ. Eng.–Geotech. Eng.*, Vol. 158, No. 2, pp. 63–73.

Osterberg, J. O., 1989, "Breakthrough in Load Testing Methodology," *Found. Drill.*, Vol. 28, No. 8, pp. 13–18.

Prasad, Y. V. S. N. and Chari, T. R., 1999, "Lateral Capacity of Model Rigid Piles in Cohesionless Soil," *Soils and Foundations (Japanese Geotechnical Society)*, Vol. 39, No. 2, pp. 21–29.

Wang, S.-T. and Reese, L., 1993, "COM624P—Laterally Loaded Pile Analysis Program for the Microcomputer, Version 2.0," *FHWA Publication No. FHWA-SA-91-048*, FHWA, Washington, D.C.